Advances in Radiation Oncology (2018) **3**, 130–138

advances
in radiation oncology

www.advancesradonc.org

Scientific Article

Serum cytokine profiles and metabolic tumor burden in patients with non-small cell lung cancer undergoing palliative thoracic radiation therapy

Hanne A. Eide MD [a,b], Ingerid Skjei Knudtsen MSc [c,d], Vandana Sandhu PhD [a], Ayca M. Løndalen MD [e], Ann Rita Halvorsen MSc [a], Azadeh Abravan MSc [c,d], Elin H. Kure PhD [a,f], Trond V. Bogsrud MD, PhD [e,g], Odd Terje Brustugun MD, PhD [a,h], Jon Amund Kyte MD, PhD [a,i], Eirik Malinen PhD [c,d], Åslaug Helland MD, PhD [a,b,j,*]

[a] *Department of Cancer Genetics, Institute for Cancer Research, Oslo University Hospital–The Norwegian Radium Hospital, Oslo, Norway*
[b] *Department of Oncology, Oslo University Hospital–The Norwegian Radium Hospital, Oslo, Norway*
[c] *Department of Physics, University of Oslo, Oslo, Norway*
[d] *Department of Medical Physics, Oslo University Hospital, Oslo, Norway*
[e] *Department of Radiology and Nuclear Medicine, Oslo University Hospital, Norway*
[f] *Department of Natural Sciences and Environmental Health, University College of Southeast Norway, Bø in Telemark, Norway*
[g] *Department of Nuclear Medicine and PET-Centre, Aarhus University Hospital, Aarhus, Denmark*
[h] *Section of Oncology, Drammen Hospital, Vestre Viken Hospital Trust, Drammen, Norway*
[i] *Department for Cell Therapy, Oslo University Hospital–The Norwegian Radium Hospital, Oslo, Norway*
[j] *Institute of Clinical Medicine, University of Oslo, Norway*

Received 19 December 2017; accepted 20 December 2017

Abstract

Purpose: Radiation therapy effectively kills cancer cells and elicits local effects in the irradiated tissue. The aim of this study was to investigate the kinetics of cytokines in the serum of patients with lung cancer undergoing radiation therapy and to identify associations with metabolic tumor burden as determined by 2-deoxy-2-fluoro-D-glucose (^{18}F-FDG) positron emission tomography (PET).

Methods and materials: Forty-five patients with advanced non-small cell lung cancer were included in a phase 2 clinical trial and randomized between fractionated thoracic radiation therapy alone or concurrent with an epidermal growth factor receptor inhibitor. Blood was sampled at 4 different time points: prior to treatment, midtherapy, at the end of therapy, and 6 to 8 weeks after

Conflicts of interest: The authors have no conflicts of interest to disclose.
Sources of support: This work was supported by the The Norwegian Cancer Society and the Regional Health Authorities in the South East of Norway.
* Corresponding author. Oslo University Hospital–The Norwegian Radium Hospital, Postboks 4953 Nydalen, 0424 Oslo, Norway.
E-mail address: ahelland@medisin.uio.no (Å. Helland).

https://doi.org/10.1016/j.adro.2017.12.007

the start of treatment. The serum concentrations of 48 cytokines and 9 matrix metalloproteinases were measured with multiplex immunoassays. A subset of patients was examined by ^{18}F-FDG PET/computed tomography before, during, and after radiation therapy. The maximum standardized uptake values (SUV_{max}) of the primary lung tumor, whole-body metabolic tumor volume, and total lesion glycolysis were calculated, and correlations between the PET parameters and cytokines were investigated.

Results: The SUV_{max} decreased from baseline through midtherapy to posttherapy ^{18}F-FDG PET/computed tomography ($P = .018$). The serum levels of C-C motif chemokine ligand (CCL) 23, CCL24, C-X3-C motif chemokine ligand 1, and interleukin-8 (C-X-C motif ligand [CXCL]8) were significantly correlated to SUV_{max}, metabolic tumor volume, and total lesion glycolysis before, during, and after radiation therapy. CXCL2 ($P = .030$) and CXCL6 ($P = .010$) decreased after the start of therapy and changed significantly across the sample time points. Serum concentrations of CCL15 ($P = .031$), CXCL2 ($P = .028$), and interleukin-6 ($P = .007$) were positively correlated to the irradiated volume during the second week of treatment.

Conclusions: Cytokine serum levels vary and correlate with metabolic tumor burden in patients with advanced non-small cell lung cancer undergoing palliative thoracic radiation therapy.

Introduction

Lung cancer is one of the most common types of cancers and the number-one cause of cancer-related death worldwide.[1] Non-small cell lung cancer (NSCLC) represents 80% to 85% of all lung cancer cases, and the treatment and prognosis largely depend on the disease stage at the time of diagnosis. Patients with advanced disease have a poor prognosis because the illness is beyond the possibility of curative treatment. The treatment of advanced NSCLC includes systemic chemotherapy, immunotherapy, and/or targeted therapy. In addition, many patients will benefit at some point from radiation therapy.

Radiation therapy affects living cells by inducing DNA damage and the loss of clonogenic potential.[2] However, the targeted tumor is not merely a collection of malignant cells; it is infiltrated by tumor-associated fibroblasts, tumor vasculature/lymphatic system, and immune cells, which are also affected by the irradiation. It is evident that the tumor microenvironment plays an important part in the response to treatment.[3,4] Indeed, tumor irradiation will lead not only to cancer cell death but also induce cascades of cellular processes that trigger angiogenesis and inflammatory cell recruitment, remodeling of the extracellular matrix, and processes that affect tumor metabolism.[5,6]

A switch to a glycolytic metabolism, the so-called Warburg effect, is favored in many tumor types.[7] A combination of 2-deoxy-2 (^{18}F) fluoro-D-glucose (FDG) positron emission tomography (PET) and computed tomography (CT) exploits this cellular trait and enables the visualization and quantification of the glucose metabolism in tumors. The maximum standardized uptake value (SUV_{max}) is the relative tracer uptake in 1 voxel with the highest uptake within a region or volume of interest that is selected by the interpreter.[8] Other metrics for analysis of tumor FDG uptake include metabolic tumor volume (MTV) and total lesion glycolysis (TLG). These are typically reported as the MTV/TLG of a single lesion or the total MTV/TLG within the patient.[8] Several studies have assessed the changes in ^{18}F-FDG uptake during radiation therapy, and differences in responders and nonresponders have been reported.[9-11] The intrinsic molecular processes within the irradiated tumor, or rather within the treated patient, that these changes represent and how they affect treatment outcome remain largely unknown.

Cytokines are soluble polypeptides that participate in cell-to-cell communication, either affecting neighboring cells in a paracrine manner or distant cells by autocrine mechanisms. Cytokines are important components in the promotion of neoplastic growth but also are known to act as biologic modulators after cancer treatment.[12] Radiation therapy will induce immediate responses in the irradiated tissue, with an increased expression of cytokines instrumental in generating free radicals and oxidative stress, as well as cytokines striving to restore homeostasis.[13] Thus, cytokines have the potential to affect cellular radiation sensitivity, and cytokine levels in circulation may mirror the biologic changes induced by radiation therapy.

In this paper, the levels of circulating cytokines and matrix metalloproteinases (MMP) in serum and whole-body glycolytic metabolic activity were investigated in patients with advanced NSCLC before, during, and after a course of radiation therapy. The objectives of this study were to elucidate associations between cytokines/MMPs and ^{18}F-FDG PET/CT parameters during treatment to unravel treatment-associated mechanisms.

Methods and materials

Study population and data collection

Forty-five patients with advanced NSCLC were included in an open-label, randomized, phase 2, clinical trial

entitled the Thoracal Radiotherapy and Tarceva (ThoRaT) study at Oslo University Hospital, Norway. Patients were randomized to external beam fractionated radiation therapy 3 Gy × 10 alone or combined with a daily, orally administered epidermal growth factor receptor (EGFR) inhibitor, erlotinib (Tarceva; Roche) throughout the radiation therapy treatment (Supplementary Figure S1). Patients with all types of NSCLC histologies were allowed in the study, as were patients who had received prior systemic therapy. There were no EGFR mutations present in the nonsquamous lung tumors. Other eligibility criteria included Eastern Cooperative Oncology Group status of 0-2 and adequate hepatic, renal, and bone marrow function. Treatment after radiation therapy was permitted in accordance with the national guidelines for treatment of lung cancer.

The baseline characteristics of the 45 patients with NSCLC are listed in Table 1. NSCLC disease was staged in accordance with the Union for International Cancer Control TNM Classification of Malignant Tumors, 7th edition. Histopathologic evaluations were collected from pathology reports. The clinical information and results from laboratory blood analyses were recorded at regular visits to an oncologist before, during, and after treatment completion. All data were registered in a database established for the project.

Table 1 Patient characteristics

Characteristic	Number (n = 45)	%
Age at inclusion (y), median (range)	69 (47-88)	
Randomized to group		
Radiation therapy	22	48.9
Radiation therapy and erlotinib	23	51.1
Sex		
Male	32	71.1
Female	13	28.9
Smoking history		
Current	13	28.9
Former	32	71.1
Pack-years		
Median (range)	30 (4-144)	
Performance status at baseline		
0	8	17.8
1	22	48.9
2	15	33.3
Stage		
III	12	26.7
IV	33	73.3
Histology		
Adenocarcinoma	26	57.8
Squamous cell carcinoma	14	31.1
Not otherwise specified	5	11.1
Previous chemotherapy		
Yes	17	37.8
No	28	62.2
Steroids during radiation therapy		
Yes	15	33.3
No	30	66.7

Treatment protocol

Radiation therapy (3 Gy × 10) was administered by 2 opposing anterior-posterior/posterior-anterior 6 MV photon beams encompassing the primary tumor (gross tumor volume) plus margins covering subclinical disease, respiratory motion, and patient setup variations. In a majority of the patients, parts of the mediastinum were included in the irradiated field, either because of verified metastases or suspected microscopic disease. The irradiated volume was estimated as the area receiving >90% of the maximum dose (cm^3).

Blood sample processing

Patient samples were collected at 4 time points: at inclusion, during the first and second weeks of radiation therapy, and 6 to 8 weeks after the initiation of radiation therapy. Blood samples were collected in serum tubes, stored at room temperature for coagulation, and spun at 2450 g for 15 minutes within 1 hour of sampling. The samples were transferred into 250 μL aliquots (cryovials) and stored at −80°C until analysis.

The sample set consisted of 43 serum samples taken before radiation therapy, including 42 and 35 samples taken the first and second week of radiation therapy, respectively, and 25 samples taken at 6 to 8 weeks. A total of 19 patients completed blood tests at all 4 time points and 31 patients at the first 3 time points. The median irradiation dose delivered in the first week of serum sampling was 9 Gy (range, 6-24 Gy); median does in the second week 24 Gy (range, 21-30 Gy).

Cytokine analysis

The serum levels of the 48 cytokines and 9 MMPs (Table 2) were quantified with a multiplex bioassay (BioRad, Hercules, CA) in accordance with the manufacturer's instructions, as previously described.[14] Concentrations were calculated using an 8-parameter standard curve. All samples were assayed in duplicate and averaged to calculate concentrations in the serum. Serum sampled at different time points in individual patients was included on the same assay plate.

^{18}F-FDG PET/CT

The ^{18}F-FDG PET/CT was used in a subset of patients at 3 time points: before radiation therapy, during the course of radiation therapy (midtherapy), and 6 to 8 weeks after

Table 2 Complete list of cytokines and MMPs

CCL1 (C-C motif chemokine ligand 1/I-309)
CCL2 (monocyte chemotactic chemokine-1)
CCL3 (macrophage inflammatory protein-1 alpha)
CCL5 (RANTES)
CCL7 (monocyte chemotactic chemokine-3)
CCL8 (monocyte chemotactic chemokine-2)
CCL11 (eotaxin)
CCL13 (monocyte chemotactic chemokine-4)
CCL15 (macrophage inflammatory protein-1 sigma)
CCL17 (thymus and activation regulated cytokine)
CCL19 (macrophage inflammatory protein-3 beta)
CCL20 (macrophage inflammatory protein-3 alpha)
CCL21
CCL22 (macrophage derived chemokine)
CCL23 (myeloid progenitor inhibitory factor-1)
CCL24 (eotaxin-2)
CCL25 (thymus expressed cytokine)
CCL26 (eotaxin-3)
CCL27
CXCL1 (growth-regulated protein alpha)
CXCL2 (Growth-regulated protein beta)
CXCL5
CXCL6 (granulocyte chemotactic protein-2)
CXCL9 (monokine induced by gamma interferon)
CXCL10 (interferon gamma induced protein-10)
CXCL11 (interferon inducible T-cell alpha chemoattractant)
CXCL12 (stromal-derived factor 1 alpha + beta)
CXCL13
CX3CL1 (fractalkine)
IL-1b
IL-1ra
IL-2
IL-4
IL-6
IL-8 (CXCL8)
IL-10
IL-12p70
IL-16
IL-17a
SCYB16
Interferon gamma (IFNγ)
Tumor necrosis factor alpha (TNFα)
Tumor necrosis factor-related apoptosis-induced ligand (TRAIL)
Macrophage migration inhibitory factor (MIF)
Granulocyte-colony stimulating factor (G-CSF)
Granulocyte-macrophage colony-stimulating factor (GM-CSF)
Platelet-derived growth factor subunit B (PDGF-BB)
Vascular endothelial growth factor (VEGF)
MMP-1
MMP-2
MMP-3
MMP-7
MMP-8
MMP-9
MMP-10
MMP-12
MMP-13

CCL, C-C motif chemokine ligand; CXCL, C-X-C motif chemokine ligand; CX3CL1, C-X3-C motif chemokine ligand 1; IL, interleukin; MMP, matrix metalloproteinase.

the start of treatment. All examinations were performed on the same PET/CT scanner (Siemens Biograph 16, Siemens Healthcare, Erlangen, Germany) with standard clinical acquisition and reconstruction protocols. Images were reconstructed using an iterative reconstruction with 2 iterations and 6 subsets. The 3.5 mm image pixel size was displayed in a 168×168 matrix array. Emission data were corrected for scatter, random events, and dead-time losses using the manufacturer's standard software and postreconstruction. A Gaussian smoothing filter with a full width half maximum of 5 mm was applied to the images.

The CT images without contrast were obtained from helical volume mode scanning (rotation time: 0.5 seconds; pitch: 0.75; tube voltage: 120 kV; quality reference mAs: 50 for integral automatic exposure control [CareDose]; slice thickness: 5 mm; distance between slices: 3 mm) were automatically fused with the PET images. The patients fasted for at least 6 hours, and blood sugar levels were determined before the intravenous administration of 370 MBq FDG. The following criteria need to be met for the PET examination to be included in the study: 1) blood glucose level <11 mmol/L,[8] 2) time between radiotracer injection and image acquisition at 55 to 75 minutes, and 3) the time difference between radiotracer injection and image acquisition for each patient on different imaging sessions was within ±10 minutes. No correction was applied for blood glucose level. The patients were imaged from the vertex to the proximal thighs.

The PET/CT scans were evaluated by nuclear medicine physicians. A radiation oncologist delineated the primary lung tumor (gross tumor volume) based on baseline PET/CT and diagnostic CT scans. The PET/CT images were transferred to an external computer and analyzed with in-house-developed software in IDL, version 8.5 (Exelis Visual Information Solutions Inc.; Harris Corporation, Boulder, CO). The voxel values in the PET images were represented as SUVs that were normalized to body weight. For each pathologic lesion, the metabolic tumor volume (MTV_l) was calculated as the volume of all voxels with SUV >2.5[15] and SUV >41% of $SUV_{max,\ lesion}$[8] while the total lesion glycolysis (TLG_l) was calculated as $MTV_l \times SUV_{mean,MTV.}$ Whole-body MTV/TLG was further calculated by summation of MTV/TLG from all malignant lesions. SUV_{max} of the primary tumor was extracted for each patient and imaging session.

The PET/CT was performed prior to radiation therapy in 15 patients, midtherapy in 25 patients, and at 6 to 8 weeks in 15 patients. All patients with PET/CT before the start of therapy also had blood samples available for cytokine analyses. Furthermore, 20 of 25 patients and 14 of 15 patients had PET/CT and blood samples at midtherapy and at 6 to 8 weeks, respectively. Eight patients completed PET/CT scans at all consecutive time points. The midtherapy PET/CT was performed at a median irradiation dose of 18 Gy (range, 12-24 Gy).

Statistical analysis

Data were reported using descriptive statistics with percentages, means, medians, and ranges. Nonparametric tests (Mann-Whitney U/Kruskal-Wallis) were used to investigate differences in the distributions of cytokine concentrations in serum. A comparison of cytokine concentration changes in different groups over time was analyzed with a 2-way analysis of variance. Correlation analyses were performed using Pearson or Spearman tests where appropriate. The correlation analyses of PET/CT values and cytokine concentrations are presented as merged, but the analyses were made separately at corresponding time points for all cytokines. SPSS software, version 21 (SPSS, Inc.; Chicago, IL) and R, version 3.2.2 (R Project for Statistical Computing, Vienna, Austria) were used for the analyses. Two-sided *P*-values <.05 were considered statistically significant. The analyses in this paper were considered hypothesis-generating.

Ethical considerations

Patients who were included in this study signed a written consent to participate. The project was approved by the Regional Ethics Committee in South-East of Norway (reference number 2012/320) and by the Radium Hospital internal review board.

Results

The median level of SUV_{max} and TLG decreased from baseline through midtherapy to posttherapy ^{18}F-FDG PET (Supplementary Table S1). MTV had a peak median value at midtherapy PET. Only SUV_{max} decreased significantly throughout treatment ($P = .018$). Figure 1 shows ^{18}F-FDG PET/CT images of a patient with a clear reduction in SUV_{max}, MTV, and TLG from pretherapy to midtherapy imaging section. Six weeks after therapy, the tumor ^{18}F-FDG uptake is only slightly above the blood background level. Of note, this patient did not receive additional erlotinib.

The levels of C-C motif chemokine ligand (CCL) 23, CCL24, C-X3-C motif chemokine ligand 1 (CX3CL1), and interleukin (IL) 8 (C-X-C motif ligand [CXCL]8) were significantly correlated to SUV_{max}, MTV, and TLG at all corresponding time points (Table 3, Figs 2 and S2). Platelet-derived, growth factor subunit B levels were significantly correlated with SUV_{max}, but CCL20 and IL-6 were significantly correlated with TLG at all time points.

Table 3 Correlations between 2-deoxy-2-fluoro-D-glucose positron emission parameters and cytokine/matrix metalloproteinase serum levels

Cytokines	SUV_{max} CC (*P*-value)	MTV CC (*P*-value)	TLG CC (*P*-value)
CCL20			0.28 (.040)
CCL23	0.30 (.040)	0.55 (4.6e-05)	0.53 (.0001)
CCL24	0.30 (.040)	0.50 (.0003)	0.46 (.0008)
CX3CL1	0.29 (.040)	0.40 (.005)	0.39 (.005)
IL-6			0.35 (.010)
IL-8 (CXCL8)	0.35 (.010)	0.32 (.020)	0.40 (.004)
PDGF-BB	0.29 (.040)		

Only cytokines that show significant associations with any of the positron emission tomography parameters are shown.
CC, correlation coefficient; CCL, C-C motif chemokine ligand; CX3CL1, chemokine C-X3-C chemokine motif ligand 1; IL, interleukin; MTV, metabolic tumor volume; PDGF-BB, platelet-derived growth factor subunit B SUVmax, maximum standardized uptake value; TLG, total lesion glycolysis.

Two of the 57 cytokines/MMPs measured had a significant change in serum levels across all 4 time points evaluated in the study: CXCL2 ($P = .030$) and CXCL6 ($P = .010$; Figs 3 and S3). The concentration of CXCL2 decreased from the serum level measured at the start of radiation therapy throughout treatment to the lowest level, measured at 6 to 8 weeks after treatment. CXCL6 levels decreased during treatment to the lowest concentration level, registered at week 2 of radiation therapy, followed by a slight increase at 6 to 8 weeks. These changes were not dependent on the use of steroids or on whether the patients had received concomitant erlotinib during the radiation therapy treatment (data not shown). The concentration levels of all cytokines/MMPs evaluated at the individual time points are listed in Supplementary Table S2.

CCL3 and MMP-8 levels measured during the second week of treatment were significantly higher (*P*-values of

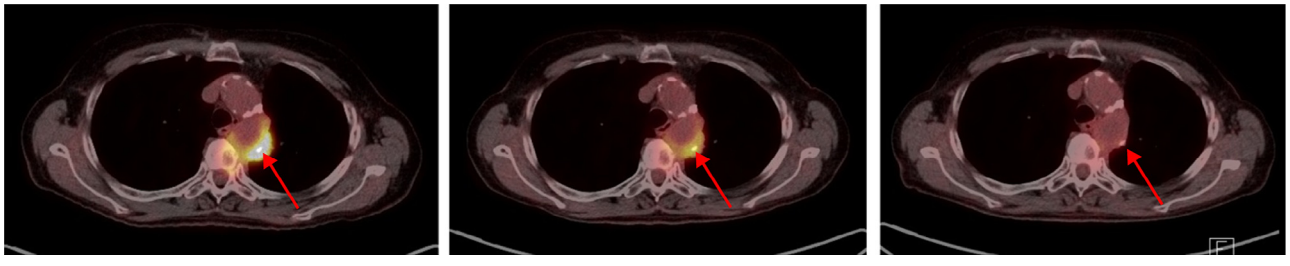

Figure 1 The 2-deoxy-2-fluoro-D-glucose positron emission tomography images of a patient showing the primary tumor (red arrow) before radiation therapy (maximum standardized uptake values [SUV_{max}]: 16 [left]), midtherapy (SUV_{max}: 6.5 [middle]), and 6 weeks after the end of therapy (SUV_{max}: 3.3 [right]). This patient was treated with radiation therapy without the addition of erlotinib.

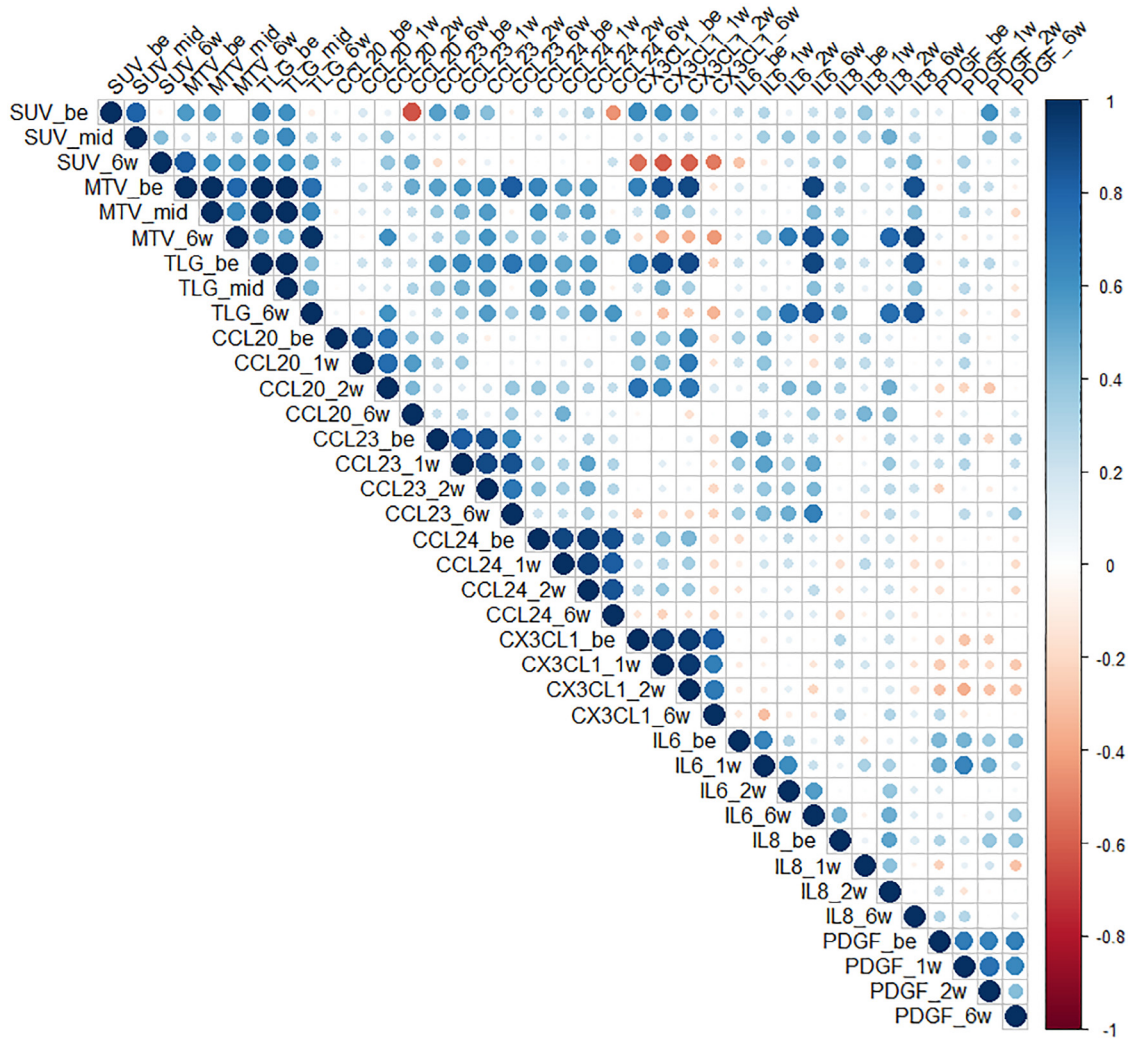

Figure 2 Correlation matrix that depicts the 2-deoxy-2-fluoro-D-glucose positron emission parameters, maximum standardized uptake values, metabolic tumor volume, and total lesion glycolysis before (be), midtherapy (mid), and 6 weeks after therapy (6w) and significantly correlated cytokines at individual time points before therapy (be), during the first (1w) and second (2w) weeks of therapy, and 6 weeks after therapy (6w). Positive correlations are displayed in blue and negative correlations in red. The intensity of color and the size of dots are proportional to the correlation coefficients.

.014 and .037, respectively) in patients receiving erlotinib in addition to radiation therapy compared with patients receiving radiation therapy alone. MMP-7 levels were significantly lower in the erlotinib group ($P = .008$; Supplementary Table S3).

The median irradiated volume from all patients was 748 cm^3 (range, 84-3382 cm^3). During the second week of treatment, the serum concentrations of CCL15 ($r = .377$; $P = .031$), CXCL2 ($r = .383$; $P = .028$), and IL-6 ($r = .459$; $P = .007$) were positively correlated with the irradiated volume.

Discussion

^{18}F-FDG PET/CT is an imaging modality that provides measurement of tracer uptake and how it varies both spatially and temporally. SUV_{max} is a single voxel measurement and does not necessarily represent the metabolic tumor burden; it may also be adversely affected by noise. Thus, other metrics for analysis of tumor FDG uptake, including MTV and TLG, may be more relevant. Indeed, high levels of MTV and TLG were associated with a poor prognosis in patients with NSCLC in previous studies.[16-18]

In this study, SUV_{max} in the tumors decreased from baseline to posttherapy, which is indicative of reduced metabolic activity in the irradiated tumors. Whole-body MTV and TLG did not change significantly, encompassing additional disease that was not directly targeted by the local radiation therapy treatment. However, there was substantial interpatient variation in the PET parameters. For example, from pre- to midtherapy PET, the changes in MTV ranged from a –48% volume reduction to a +55% volume increase. This indicates that for advanced stage NSCLC, early changes in PET

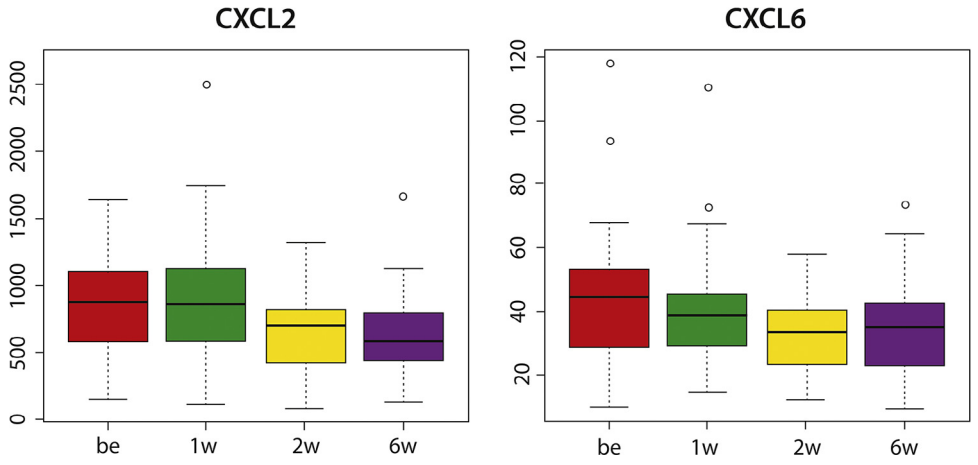

Figure 3 Serum concentration of C-X-C motif ligand (CXCL) 2 and CXCL6 measured at baseline, during the first and second weeks of treatment, and 6 to 8 weeks after the start of treatment. Cytokine serum concentrations are measured in pg/mL.

parameters may identify responders. Indeed, other studies have observed that changes in SUV_{max} and MTV measured during radiation therapy were predictive factors of treatment response.[9-11,19] However, the patients with NSCLC in these studies were treated with different radiation therapy regimes with regard to total dose and fractionation and with curative intent, contrary to our study.

The effects of radiation therapy visualized by ^{18}F-FDG PET/CT correlated with serum levels of CCL23, CCL24, CX3CL1, and IL-8 during the course of treatment. CCL23 and CCL24 are both released by macrophages and activated T-lymphocytes and attract resting T-lymphocytes, eosinophils, and, to a lesser extent, neutrophils.[20] The soluble form of CX3CL1 has chemoattractant activity for T-cells and monocytes but has no effect on neutrophils.[21] In contrast, IL-8 remains the primary cytokine involved in the recruitment of neutrophils.[22]

The ^{18}F-FDG PET signal in a tumor reflects the metabolism in both malignant cells and cells that compose the tumor microenvironment. Radiation therapy leads to cell death but also to an increased influx of macrophages and other immune cells that constitute "competing processes." These processes result in either increased or decreased ^{18}F-FDG PET signals in the irradiated tissue, both putatively indicative of tissue radiation sensitivity.

Thus, cytokines may elucidate the treatment-associated mechanisms, perhaps explaining treatment effect and consequently the prognostic/predictive value of metabolic tumor burden in patients with NSCLC. Notably, cytokine levels were correlated to a higher degree with MTV and TLG than with SUV_{max}. Whole-body MTV/TLG examined in this cohort also reflected tumor tissue that was not irradiated but capable of releasing cytokines. It is known that localized radiation therapy can trigger systemic antitumor effects, and the clinical implication of our findings warrants further investigation.

The release of cytokines after radiation therapy has been documented in previous studies, both in vitro and in vivo. Desai et al demonstrated the secretion of cytokines IL-1b, IL-1ra, IL-6, IL-8, IL-15, CX3CL1, CCL2, CXCL10, platelet-derived growth factor-AA, tumor necrosis factor (TNF) α, transforming growth factor β, vascular endothelial growth factor, granulocyte-colony stimulating factor, and granulocyte-macrophage colony-stimulating factor in a dose-dependent manner in cell line studies.[23]

In vivo, irradiation elicits a complex response with crosstalk between several actors within the tumor microenvironment as well as tumor cells, which is possibly reflected in the systemic levels of cytokines. Previous studies on radiation therapy in patients with NSCLC found stable levels of several cytokines such as IL-1, IL-6, IL-10, and TNFα throughout courses of radiation therapy, concurrent with our results.[24,25] In contrast, Wang et al discovered an increase in IL-6, IL-10, and soluble receptor 1 for TNF during treatment with radiation therapy in patients with NSCLC, but notably, a majority of the patients investigated in this study also received concomitant chemotherapy.[26] Our cohort consisted of patients with advanced NSCLC with a different fractionation schedule and lower total irradiation dose. Various radiation therapy regimes may have a dissimilar impact on circulating cytokine levels. A recent study found a difference in blood cytokine profiles during stereotactic body radiation therapy versus intensity modulated radiation therapy in patients with NSCLC, which supports that notion.[24]

In the current study, chemokines CXCL2 and CXCL6 varied significantly at the measured time points. Secreted by macrophages, CXCL2 is known to attract neutrophils and to be mitogenic for alveolar epithelial cells.[25] CXCL6 is secreted by cells of mesenchymal origin, pulmonary macrophages, and peripheral blood monocyte-derived macrophages.[27] CXCL6 also chemoattracts neutrophils[28] and

has been shown to promote tumor growth through an angiogenic effect in animal models.[29]

The expression of both CXCL2 and CXCL6 is found to be mediated by the transcription factor nuclear factor kappa B in tumor cells.[30] Nuclear factor kappa B is constitutively activated in several solid malignancies but also transiently induced by ionizing radiation.[31] The concentration of CXCL2 decreased in serum throughout and after the radiation therapy treatment in our study and was positively correlated with the volume of irradiated tissue. Similarly, there was a reduction in serum levels of CXCL6 during radiation therapy treatment. Whether induced by tumor cells, by cells of the tumor microenvironment, or by the normal cells of the lung tissue, there was a change during radiation therapy, suggesting less call for neutrophils and possibly reduced inflammation.

Exposure to ionizing radiation can induce an upregulation of cytokines but also activate prosurvival pathways in the irradiated tissue, such as the EGFR pathway.[32] The patients in our study who received an EGFR inhibitor in addition to radiation therapy had a higher median serum level of CCL3 and MMP-8 and a lower serum concentration of MMP-7 in the second week of irradiation compared with patients in the radiation therapy group. Preclinical studies have shown that EGFR inhibitors can increase radiation sensitivity. Interestingly, elevated CCL3 levels were recently proposed to be of importance in observed out-of-field DNA damage after local thoracic irradiation in patients with NSCLC.[33]

Conclusions

We explored serum cytokine concentrations of patients with advanced NSCLC throughout radiation therapy treatment and how they correlate with ^{18}F-FDG PET-derived measurements of metabolic tumor burden and irradiated volume. Although ^{18}F-FDG PET is an established indicator for prognosis and a promising predictor of treatment response, the biologic processes related to tumor glucose metabolism and how it changes during treatment are not fully understood. This study showed significant correlations between several cytokines and metabolic tumor burden, but the results will need to be validated in a larger cohort.

Acknowledgements

The authors thank Anne Fåne, Department for Cell Therapy, Oslo University Hospital, for valuable help with the multiplex bioassays, Dag Einar Sommervoll, NMBU and Daniel Nebdal, Department of Cancer Genetics, Institute for Cancer Research, Oslo University Hospital, for valuable help in making the figures included in this paper.

Supplementary data

Supplementary material for this article (https://doi.org/10.1016/j.adro.2017.12.007) can be found at www.practicalradonc.org.

References

1. Ferlay J, Soerjomataram I, Dikshit R, et al. Cancer incidence and mortality worldwide: Sources, methods and major patterns in GLOBOCAN 2012. *Int J Cancer*. 2014;136:E359-E386.
2. Eriksson D, Stigbrand T. Radiation-induced cell death mechanisms. *Tumor Biol*. 2010;31:363-372.
3. Balkwill FR, Capasso M, Hagemann T. The tumor microenvironment at a glance. *J Cell Sci*. 2012;125:5591-5596.
4. Murray MJ, Saini HK, Siegler CA, et al. LIN28 expression in malignant germ cell tumors downregulates let-7 and increases oncogene levels. *Cancer Res*. 2013;73:4872-4884.
5. Barker HE, Paget JT, Khan AA, Harrington KJ. The tumour microenvironment after radiotherapy: Mechanisms of resistance and recurrence. *Nat Rev Cancer*. 2015;15:409-425.
6. Leroi N, Lallemand F, Coucke P, Noel A, Martinive P. Impacts of ionizing radiation on the different compartments of the tumor microenvironment. *Front Pharmacol*. 2016;7:78.
7. Hanahan D, Weinberg RA. Hallmarks of cancer: The next generation. *Cell*. 2011;144:646-674.
8. Boellaard R, Delgado-Bolton R, Oyen WJ, et al. FDG PET/CT: EANM procedure guidelines for tumour imaging: Version 2.0. *Eur J Nucl Med Mol Imaging*. 2014;42:328-354.
9. van Baardwijk A, Bosmans G, Dekker A, et al. Time trends in the maximal uptake of FDG on PET scan during thoracic radiotherapy. A prospective study in locally advanced non-small cell lung cancer (NSCLC) patients. *Radiother Oncol*. 2007;82:145-152.
10. van Elmpt W, Öllers M, Dingemans AM, Lambin P, De Ruysscher D. Response assessment using 18F-FDG PET early in the course of radiotherapy correlates with survival in advanced stage non-small cell lung cancer. *J Nucl Med*. 2012;53:1514-1520.
11. Huang W, Zhou T, Ma L, et al. Standard uptake value and metabolic tumor volume of ^{18}F-FDG PET/CT predict short-term outcome early in the course of chemoradiotherapy in advanced non-small cell lung cancer. *Eur J Nucl Med Mol Imaging*. 2011;38:1628-1635.
12. Grivennikov SI, Greten FR, Karin M. Immunity, inflammation, and cancer. *Cell*. 2010;140:883-899.
13. Schaue D, Kachikwu E, McBride W. Cytokines in radiobiological responses: A review. *Radiat Res*. 2012;178:505-523.
14. Eide HA, Halvorsen AR, Sandhu V, et al. Non-small cell lung cancer is characterised by a distinct inflammatory signature in serum compared with chronic obstructive pulmonary disease. *Clin Transl Immunology*. 2016;5:e109.
15. Wahl RL, Jacene H, Kasamon Y, Lodge MA. From RECIST to PERCIST: Evolving considerations for PET response criteria in solid tumors. *J Nucl Med*. 2009;50:122-150.
16. Liao S, Penney BC, Wroblewski K, et al. Prognostic value of metabolic tumor burden on 18F-FDG PET in nonsurgical patients with non-small cell lung cancer. *Eur J Nucl Med Mol Imaging*. 2012;39:27-38.
17. Yoo SW, Kim J, Chong A, et al. Metabolic tumor volume measured by F-18 FDG PET/CT can further stratify the prognosis of patients with stage IV non-small cell lung cancer. *Nucl Med Mol Imaging*. 2012;46:286-293.
18. Im HJ, Pak K, Cheon GJ, et al. Prognostic value of volumetric parameters of (18)F-FDG PET in non-small-cell lung cancer: A meta-analysis. *Eur J Nucl Med Mol Imaging*. 2014;42:241-251.
19. Huang W, Fan M, Liu B, et al. Value of metabolic tumor volume on repeated 18F-FDG PET/CT for early prediction of survival in locally

advanced non-small cell lung cancer treated with concurrent chemoradiotherapy. *J Nucl Med*. 2014;55:1584-1590.
20. Patel VP, Kreider BL, Li Y, et al. Molecular and functional characterization of two novel human C-C chemokines as inhibitors of two distinct classes of myeloid progenitors. *J Exp Med*. 1997;185:1163-1172.
21. Bazan J, Bacon KB, Hardiman G, et al. A new class of membranebound chemokine with a CX3C motif. *Nature*. 1997;385:640-644.
22. Harada A, Sekido N, Akahoshi T, Wada T, Mukaida N, Matsushima K. Essential inflammation involvement of interleukin-8 (IL-8) in acute inflammation. *J Leukoc Biol*. 2017;56:559-564.
23. Desai S, Kumar A, Laskar S, Pandey BN. Cytokine profile of conditioned medium from human tumor cell lines after acute and fractionated doses of gamma radiation and its effect on survival of bystander tumor cells. *Cytokine*. 2013;61:54-62.
24. Trovo M, Giaj-Levra N, Furlan C, et al. Stereotactic body radiation therapy and intensity modulated radiation therapy induce different plasmatic cytokine changes in non-small cell lung cancer patients: a pilot study. *Clin Transl Oncol*. 2015;18:1003-1010.
25. Wolpe SD, Sherry B, Juers D, Davatelis G, Yurt RW, Cerami A. Identification and characterization of macrophage inflammatory protein 2. *Proc Natl Acad Sci USA*. 1989;86:612-616.
26. Wang XS, Shi Q, Williams LA, et al. Inflammatory cytokines are associated with the development of symptom burden in patients with NSCLC undergoing concurrent chemoradiation therapy. *Brain Behav Immun*. 2010;24:968-974.
27. Wuyts A, Struyf S, Gijsbers K, et al. The CXC chemokine GCP-2/CXCL6 is predominantly induced in mesenchymal cells by interleukin-1beta and is down-regulated by interferon-gamma: Comparison with interleukin-8/CXCL8. *Lab Invest*. 2003;83:23-34.
28. Proost P, De Wolf-Peeters C, Conings R, Opdenakker G, Billiau A, Van Damme J. Identification of a novel granulocyte chemotactic protein (GCP-2) from human tumor cells. In vitro and in vivo comparison with natural forms of GRO, IP-10, and IL-8. *J Immunol*. 1993;150:1000-1010.
29. Van Coillie E, Van Aelst I, Wuyts A, et al. Tumor angiogenesis induced by granulocyte chemotactic protein-2 as a countercurrent principle. *Am J Pathol*. 2001;159:1405-1414.
30. Zhu YM, Bagstaff SM, Woll PJ. Production and upregulation of granulocyte chemotactic protein-2/CXCL6 by IL-1beta and hypoxia in small cell lung cancer. *Br J Cancer*. 2006;94:1936-1941.
31. Deorukhkar A, Krishnan S. Targeting inflammatory pathways for tumor radiosensitization. *Biochem Pharmacol*. 2010;80:1904-1914.
32. Chinnaiyan P, Huang S, Vallabhaneni G, et al. Mechanisms of enhanced radiation response following epidermal growth factor receptor signaling inhibition by erlotinib (Tarceva). *Cancer Res*. 2005;65:3328-3335.
33. Siva S, Lobachevsky P, MacManus MP, et al. Radiotherapy for non-small cell lung cancer induces DNA damage response in both irradiated and out-of-field normal tissues. *Clin Cancer Res*. 2016;22:4817-4826.